Scientific Research Journal,
Vol 20, No 1 (2023) 107-123
https://doi.org/10.24191/srj.v20i1.19060

SCIENTIFIC RESEARCH JOURNAL SRJ
ISSN: 1675-7009
e-ISSN: 2289-649X

Evaluation of Crosslinking Degree on the Characteristics and Performance of Membranes Formulated from Quaternized Chitosan

Abdul Aziz Mohd. Nasir[1], Norin Zamiah Kassim Shaari[1*], Nur Syazwanie Izzati Chik[1]

[1]*School of Chemical Engineering, College of Engineering, Universiti Teknologi MARA*
40450 Shah Alam, Selangor, Malaysia

**Corresponding author's E-mail: norinzamiah@uitm.edu.my*

Received: 09 August 2022
Accepted: 18 October 2022
Online First: 17 March 2023

ABSTRACT

Chitosan is a polymer produced from chitin that is insoluble in neutral or basic pH conditions. Although chitosan has good biodegradability, non-toxicity, and biocompatibility properties, it has limited applications due to its low solubility in neutral or slightly alkaline conditions. Quaternization came out as a way of altering this natural polymer to enhance its solubility over a wide pH range and boost permanent positive charges. In this study, the quaternized chitosan (QCs) was prepared by using 3-chloro-2-hydroxypropyltrimethyl ammonium chloride (CHTAC) as the quaternizing agent, which was then formulated into the integral membrane with a blend of polyvinyl alcohol (PVA), polysulfone (PSF), and tetraethylorthosilicate (TEOS). The membrane characterizations and performance analysis were done in terms of functional groups, surface charge, surface morphology, pure water flux analysis, and antifouling analysis. The results revealed that the incorporation of TEOS produced a dense membrane structure but did not help much in enhancing the hydrophilicity and the positive charge of membranes. Membrane from the polymer blend without TEOS was found to have better hydrophilicity, and antifouling characteristics in terms of relative flux recovery (RFR) and relative flux decay (RFD) and possessed a slightly negative charge. The dense structure of the membrane due to crosslinking process might result in a high degree of integral stability, with the additional benefit of providing more adsorption area for a potential application in the heavy metal ion removal process.

Keywords: Quaternized chitosan, Tetraethyl orthosilicate, Integral membrane, surface charge, antifouling

INTRODUCTION

In the field of separation technologies, membrane separation is one of the most widely used technologies nowadays [1]. Membrane technology has been proven to be incredibly successful on both, molecular and ionic levels of separation. Various pressure-driven membranes technologies, including reverse osmosis, forward osmosis, membrane distillation, and electric field-driven membrane technologies, such as electrodialysis, have achieved widespread use for water treatment, including water softening and separation, desalination, and solute concentration [2]. As one of the organic polymers, chitosan has been widely used in heavy metal separation process due to its amino and hydroxyl groups that adsorb the metal ion. The complexed ions will grow bigger and fill the pore size of the membrane, where the macromolecules were then prevented from flowing through the membrane but allowing microscopic water molecules to infiltrate the material. Due to its biodegradability and biocompatibility, chitosan has been widely used in various industries, including food, agriculture, biomedicine, and textiles [3]. However, chitosan's usage is limited due to its low water solubility, and possibility of having low conductivity and mechanical stability if chitosan moiety was not adequately bonded to the polymer [4].

Quaternization stands out as a method for modifying natural polymers such as chitosan to enhance their solubility across a broad pH level for widening its range of applications. Besides having a greater solubility in water, quaternization process ensures a persistent positive charge of material is achieved by converting the main amino group to a quaternary ammonium ion which also can enhance its solubility [5]. Anticoagulant activity, antibacterial as well as the ability to bind negatively charged species like *DNA* species are all improved when the amine groups in C_2 of chitosan are transformed into positive-charged quaternary salts [6]. Chitosan can be quaternized in two ways that are by interacting with alky halides, such as iodomethane or dimethyl sulfate, or by reacting with quaternary ammonium compounds. Muzzarelli and Tanfani [7] were the first researchers to synthesize quaternized chitosan by reacting it with formaldehyde and sodium borohydride to produce N, N-dimethyl chitosan (*DMC*), which was then converted to N, N, N-trimethyl chitosan through iodomethane in acetonitrile [7]. Curti et al. [8] dissolved chitosan in N-methyl pyrrolidinone in the presence of sodium hydroxide before reacting it with iodomethane. For the modification of residual free primary amino groups and certain hydroxyl groups in chitosan derivatives, the N-(3-chloro-2-hydroxypropyl) trimethylammonium chloride (*GTMAC*) has been employed as a quaternizing agent to create disaccharide quaternary ammoniums [5].

In membrane separation process, quaternized chitosan is employed due to its high solubility and flexible structure [9]. A high-hydrophilicity membrane is preferred in membrane separation to minimize membrane fouling by organic materials since it has a negative impact on membrane separation process that lies in high energy consumption, longer downtime, and reduced membrane permeability [10]. Reduced permeate flux is a common effect of membrane fouling, which occurred when particles including bacteria, and organic compounds accumulate on the porous membrane [11]. This situation requires high pressure to allow the permeation of clean water, which consequently increases the operating cost [12]. Polarization and solute adsorption can occur if the flux below critical flux (Jcrit) is controlled, although both processes are reversible and adapt rapidly to emerging in convection. A drop in flux that cannot be regained by boosting the shear rate could well be totally recovered by a momentary suspension of the permeate flow. Koltuniewicz and Noworyta used Danckwerts' surface renewal theory to describe the flux drop caused by the establishment of a concentration polarisation layer [13]. Because the membrane was not occupied by a single layer with similar permeate flow resistance as expected in the film model, the permeate was forced to flow through an unevenly aged mosaic of relatively thin elements. A hydrodynamic impulse can remove any element at irregular intervals, and a new element then began to build up a layer of residual solute in the same region on the surface of the membrane. As a result of the concentration polarisation layer being built up over time, a decrease in flux was observed [13].

Cross-linking is described as a process of modifying the physical properties of polymers through covalent or ionic interactions. Berger et al. [14] investigated the structure and chemical interactions of ionically and chemically cross-linked chitosan, where it was discovered that cross-linkers connect polymer chains to form three-dimensional networks within cross-linked chitosan. In addition to the ionic and covalent connections, chitosan networks also contain additional interactions, such as hydrophilic groups and hydrogen bridges. An alkoxysilane derivative is widely used as a cross-linker that can provide a three-dimensional inorganic (SiO_2) backbone through the formation of covalent bonds with organic polymer [14]. Cross-linking process occurs through a sol-gel method where this method ensures easily controllable concentrations of organic and inorganic to result in a homogeneous solution due to both components are dispersed at the molecular level in the membranes [15, 16].

This research aims to investigate the modification techniques of chitosan using 3-chloro-2-hydroxypropyltrimethyl ammonium chloride (CHTAC), where the quaternized chitosan was subsequently blended with polyvinyl alcohol, polysulfone and tetraethylorthosilicate (*TEOS*) to form a membrane. The effect of varying concentrations of *TEOS* on the surface charge, functional group, surface morphology, water flux, and antifouling characteristic of the formulated membranes was investigated.

METHODOLOGY

Material

Polyvinyl alcohol (PVA) with hydrolysis degree of 87 % - 89 % (MW: 85000 – 124000) pellets and dimethyl sulfoxide (*DMSO*) were purchased from Sigma-Aldrich (M) Sdn. Bhd and Aman Semesta Enterprise Sdn. Bhd respectively, Polysulfone resin pellets (MW: 44000 – 53000), commercial chitosan (deacetylation degree 84.4 ± 12 %), tetraethylorthosilicate (*TEOS*) with 99 % purity, Chloro Hydroxypropyl Trimethylammonium Chloride (*CHTAC*) were purchased from BT Science Sdn. Bhd, Potassium Hydroxide (*KOH*) pellet, Hydrochloric Acid (*HCl*) with 37 % purity as a catalyst, and NaOH were purchased from R & M Chemicals, Subang. The acetic acid solution, ethanol, polyethylene glycol (PEG 400), and N-Methyl-2-pyrrolidone (*NMP)* were purchased from Merck Sdn. Bhd.

Preparation of Quaternized Chitosan (QCs)

0.5 g of chitosan was dissolved in 99.5 g of 2 wt. % acetic acid at 90 °C under constant stirring at 400 rpm for 4 hours. The mixture was left to cool to 65 °C before the addition of 10 g *CHTAC*. Then, 15 g of KOH (1 M) solution was added to the mixture and continuously stirred at 400 rpm at 65 °C for 4 hours. The resulting solution was mixed with 400 mL of ethanol for the precipitation process, and then the solution was filtered using Smith filter paper. The white precipitates of quaternized chitosan were subsequently used in the next step.

Preparation of Polyvinyl Alcohol (PVA) Solution

A mixture of 10 g Polyvinyl Alcohol (*PVA*) and 90 mL of Dimethyl Sulfoxide was homogenized under continuous stirring at 400 rpm at 90 °C. The mixture was allowed to cool to room temperature for 6 hours.

Preparation of Hybrid Solution

Initially, a 1:10 weight ratio of *QCs* solution to *PVA* solution was used. 5 g of *QCs* precipitate was added to 50 g *PVA* solution, followed by the addition of 0.5 g *TEOS* in the mixture. 1 mL of hydrochloric acid at 37 wt. % concentration was added to the mixture to initiate the sol-gel process. The solution was heated to 40 °C and stirred at 400 rpm for 6 hours. The same procedure was repeated for 1.0 g of *TEOS* and a control solution without T*EOS*.

Preparation of Polysulfone (PSF) Solution

The *PSF* solution was made by adding 13 g of *PSF* resin pellets to 82 g of N*MP* solution, followed by the addition of 5 g of *PEG* 400. The mixture was stirred at 400 rpm for 6 hours at a temperature of 80 °C. Before mixing it with the hybrid solution, the solution was allowed to cool to ambient temperature.

Preparation of Integral Membrane

To synthesize the integral membrane, 1 g of the hybrid solution was mixed with 50 g of *PSF* solution. The mixture was then heated to 80 °C and stirred at 750 rpm for 3 hours. Before being cast into a membrane film, the mixture was left to cool at room temperature for 1 hour. Then, the solution was poured onto a glass plate and a Baker's film applicator was used to spread the solution at a thickness of 100 µm to form a film. As the phase inversion method was used, the coated glass plate was immersed immediately in a water basin. The film formed was removed from the plate and left in the water basin for 24 hours. The membrane was dried under the sun for 2 days before characterizations were performed. Table 1 depicts the formulations of the integral membranes.

Table 1: Formulations of integral membranes

Membrane Code	1 g of Hybrid Solution			*PSF* (g)
	PVA (g)	*QCs* (g)	*TEOS* (g)	
M1	50	5	0	50
M2	50	5	0.5	50
M3	50	5	1.0	50

Fourier Transform Infrared (*FTIR*) Analysis

Fourier Transform Infrared Spectroscopy (*FTIR*) Perkin – Elmer Spectrum 2000 was used to analyze the functional groups of membranes. The analysis was done at a wavelength between 400 cm^{-1} and 4000 cm^{-1}.

Zeta Potential Analysis

Zeta potential measurements were performed by using a Malvern Zetasizer Nano ZS instrument equipped with a 632 nm HeNe laser operating at a 173^o detector angle. The membrane samples were accurately cut into 2 cm × 2 cm in dimensions. Then, each piece of membrane film was immersed in a test cell containing deionized water. In a test cell, the solution's upper surface was removed after it has settled for 5 minutes. These samples were loaded into a disposable folded capillary cell. The cells have two conductive electrodes that contact the instrument's applied voltage on the outside and fold in to contact the liquid sample on the inside. The surface charge of the membranes was recorded.

Pure Water Flux (PWF) Analysis

PWF analysis was carried out using a fabricated dead-end mode of filtration rig, which uses nitrogen gas as the purging gas. The membrane was cut into a circular shape with a cross-sectional area of 19 cm^2 using a cutter. The stirred cell was filled with 300 mL of deionized water as the feed solution. By applying a 6 bars pressure of nitrogen gas and with an hour of filtration duration, the permeate sample was withdrawn at 15 minutes intervals for volume measurement. Then, the flux was calculated using Equation (1).

$$PWF = \frac{Q}{(A \times \Delta T)} \tag{1}$$

Where:
Q - Permeate volume (L)
A - Membrane cross-sectional area (m^2)
ΔT - Time (h)

Antifouling Analysis

In this antifouling test, humic acid (HA) solution was used as a foulant model to closely mimics the organic compounds in the environment. 10 bars of nitrogen gas pressure were used during the antifouling experiment [17]. There were three stages involved in the process. Initially, a humic acid solution was prepared by dissolving 2 g of humic acid in 1L of 200 ppm sodium hydroxide solution. Deionized water was used as the feed solution in the first stage of the experiment, which was completed in 30 minutes. The flux (J_o) was measured from the volume collected. In the second stage, the humic acid solution was used as the feed solution. The filtration was performed for 2 hours and the final volume was collected. The flux was calculated and recorded as J_p The membrane was backwashed by stirring at 150 rpm using a magnetic bar for 30 minutes. In the final stage, the procedure of the first stage was repeated and the final flux was recorded as J_l. Equations (2) and (3) were used to determine the antifouling properties, which were Relative Flux Decay (*RFD*) and Relative Flux Recovery (*RFR*) [18].

$$RFD = \left(\frac{J_O - J_P}{J_O}\right) \times 100 \tag{2}$$

$$RFR = \left(\frac{J_1}{J_O}\right) \times 100 \tag{3}$$

Field Emission Scanning Electron Microscope (*FESEM*) Analysis

To examine the morphology of the membrane, a *FESEM* instrument (Hitachi S-4800, Japan) was used. Each sample of the membrane was coated with gold using ion sputtering before being scanned and photographed. During image acquisition, the accelerating potential was set at 5 kV and the magnification was set at approximately 10,000 x. The images for each membrane were recorded.

RESULT AND DISCUSSIONS

Fourier Transform Infrared Spectroscopy (*FTIR*) Analysis

Figure 1 demonstrated the *FTIR* spectra for the formulated membranes. For membrane M1 with quaternized chitosan and without cross-linking process, existence of quaternary ammonium salt group on chitosan backbone at peaks 953 cm^{-1} and 1737 cm^{-1} respectively justifies the occurrence of C=O bond of the ester group and C-N bond from quaternary ammonium group [19]. Peaks corresponding to the chitosan structure at 1655 cm^{-1}, and 1595 cm^{-1} that represents the main amine group have diminished for all membranes [20]. This was due to the transformation of primary amine into secondary amine during quaternization process [19]. The peak at 3400 cm^{-1} corresponds to -OH absorbance, where it exhibits the hydrophilicity of a membrane. It was observed from Figure 1 that membrane M1 has high hydrophilicity as compared to membranes M2 and M3 which exhibited a higher intensity of the peak. Regarding the crosslinking process with TEOS, the peak corresponding to the Si-O-C bond appeared at 1100 cm^{-1} for M2 and M3, which overlapped the C-O bond of the polyvinyl alcohol for M1 [21]. A higher concentration of TEOS resulted in higher intensity of the peak as observed for M3.

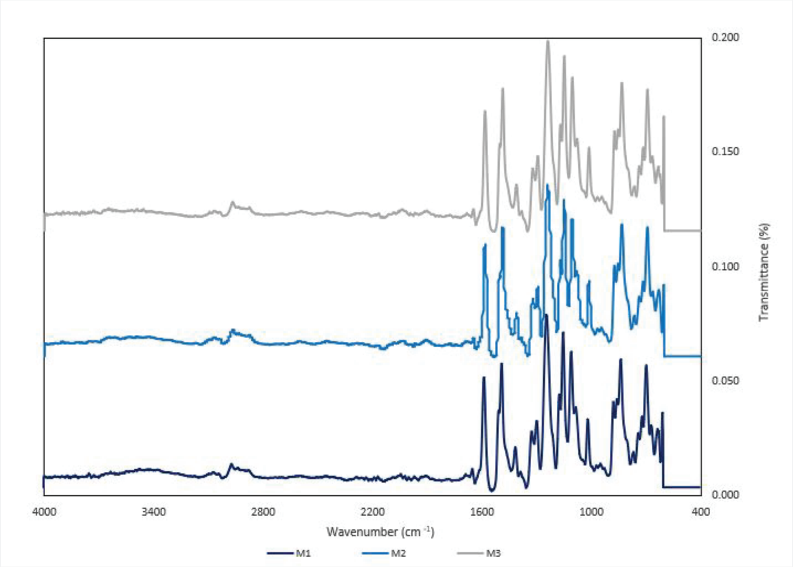

Figure 1: FTIR spectra of M1, M2, and M3.

Zeta-Potential Analysis

Table 2 shows the surface charges for all membranes that were generated from zeta potential analysis. Relative to charge of deionized water without membrane (control solution), all membranes demonstrated negative charges where the value proportionally increased with the concentration of *TEOS* incorporated in the membrane. This phenomenon can be related to the report by Wang *et al.* [22] where silica nanoprecursor from *TEOS* has a negative charge that resulted in membranes with higher negative charges after it was blended with a negatively charged polymer blend (M1). Weight ratio of *QCs* to *TEOS* also influenced the surface charge values, where the decrease in the *QCs/TEOS* weight ratio resulted in a decrease in the surface charge due to cross-linking interaction between *TEOS* and amino groups on the *QCs* chain, which resulted in the reduction of residual amine groups of *QCs* [22].

Table 2: The average values of surface charges from all membranes

Sample	*Temperature (°C)*	*ZP (mV)*	*pH*
Control solution (without membrane)	25	-10	7.15
M1	25	-13.87	7.15
M2	25	-18.63	7.15
M3	25	-24.93	7.15

Pure Water Flux (PWF) Analysis

Results of water flux for all membranes are shown in Figure 2. Membrane M1 formulated from quaternized chitosan has the highest flux throughout the 1-hour filtration process. It was expected that membranes M2 and M3 have denser structures resulting from the crosslinking process with *TEOS* [23]. Without the crosslinking process, and with a reduction in crystallinity structure of quaternized chitosan, membrane M1 was anticipated to have a large pore size that contributed to higher flux [24]. This result shows similar trend as observed in a previous research by Heidari et al. [25].

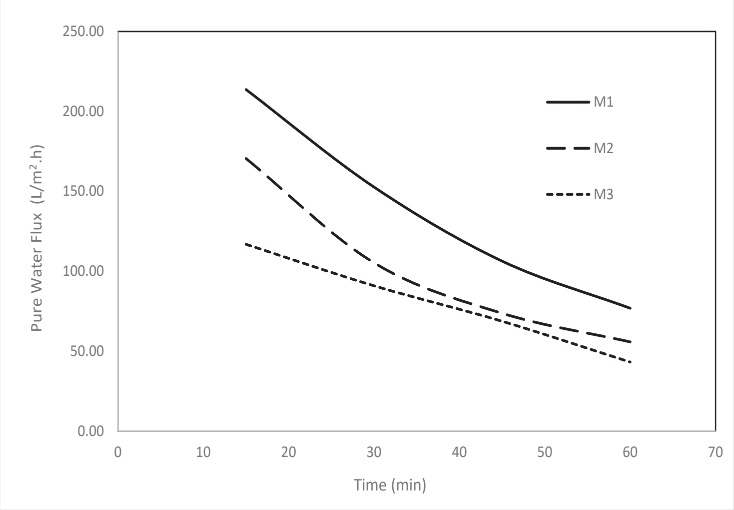

Figure 2: Pure water flux of membranes

Antifouling Analysis

Table 3 demonstrates the values of J_o, J_P, and J_I for all membranes. Accordingly, all membranes depicted a drastic flux declining rate during the HA filtration as being displayed through J_P value as compared to when deionized water was used as the feed solution (J_O). All membranes exhibited high RFR, which can be related to good surface hydrophilicity. During the 3-hour filtration period, membrane M1 had the highest flux, regardless of the type of solution used. Furthermore, it has the lowest relative flux decay (*RFD*). Although the highest *RFR* was observed for membrane M3, but it suffers from the highest *RFD*.

Membrane fouling is influenced by hydrodynamic circumstances and physical surface morphology of a membrane that covers its porous structure, and chemical interactions between the membrane material and foulants [25]. The increased adhesion between the membrane material and collagen particles enhanced the foulant deposition on the membrane surface, resulting in the formation of a denser cake layer [26]. Due to a greater adhesive force, this layer is substantially harder to eliminate from the membrane surface resulting in flux decay, and poor permeability recovery [25]. This is where surface hydrophilicity plays an important role to enhance the antifouling characteristics. Therefore, utilizing various polymers as the membrane materials enforce changes in physicochemical qualities and membrane surface morphologies, which were likely responsible for the antifouling properties. Furthermore, the antifouling characteristic of a membrane seemed to be mostly attributable to the greater effect of membrane material on the properties of the fouling layer than the effect of its porous structure [26]. The results from Table 3 have proven that the formulated quaternized chitosan has enhanced the surface hydrophilicity of the membranes.

Table 3: Antifouling characteristics of membranes

Membrane Code	J_o	J_P	J_1	*RFD (%)*	*RFR (%)*
M1	102	49.3	92	51.67	90.20
M2	98	40.5	80	57.50	81.63
M3	95	33.6	88	67.79	92.63

Field Emission Scanning Electron Microscope (*FESEM*) Analysis

Figure 3 displays the *SEM* images of the surface morphology for all membranes. Membrane M1 has a smooth surface and the pore size ranges from around 0.43 to 0.53 µm. After the crosslinking process with 0.5 wt. % *TEOS*, it was observed that M2 has a slightly reduced pore size compared to M1. A smaller pore size of 65.4-73.6 nm was observed for membrane M3, which was attributed to a rapid crosslinking process between hydroxyl groups from polymer with Si-OH bond from *TEOS*. This smaller pore size will result in more surface area for the adsorption process, which is preferable for metal ions adsorption for instance.

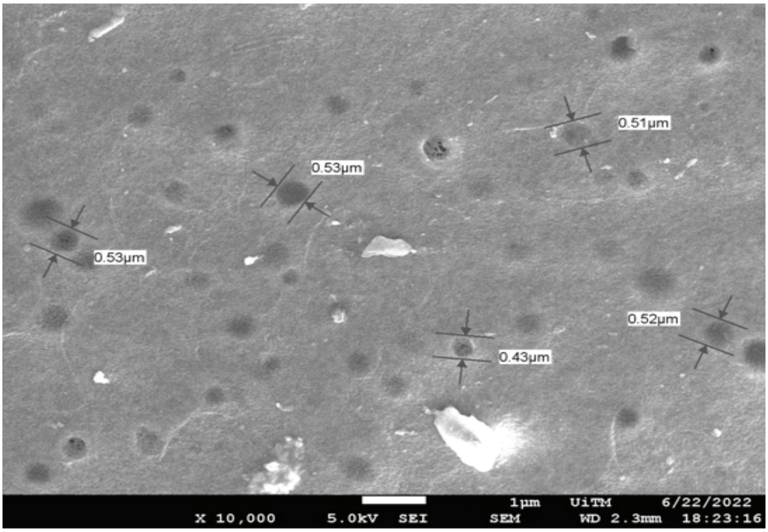

(a)

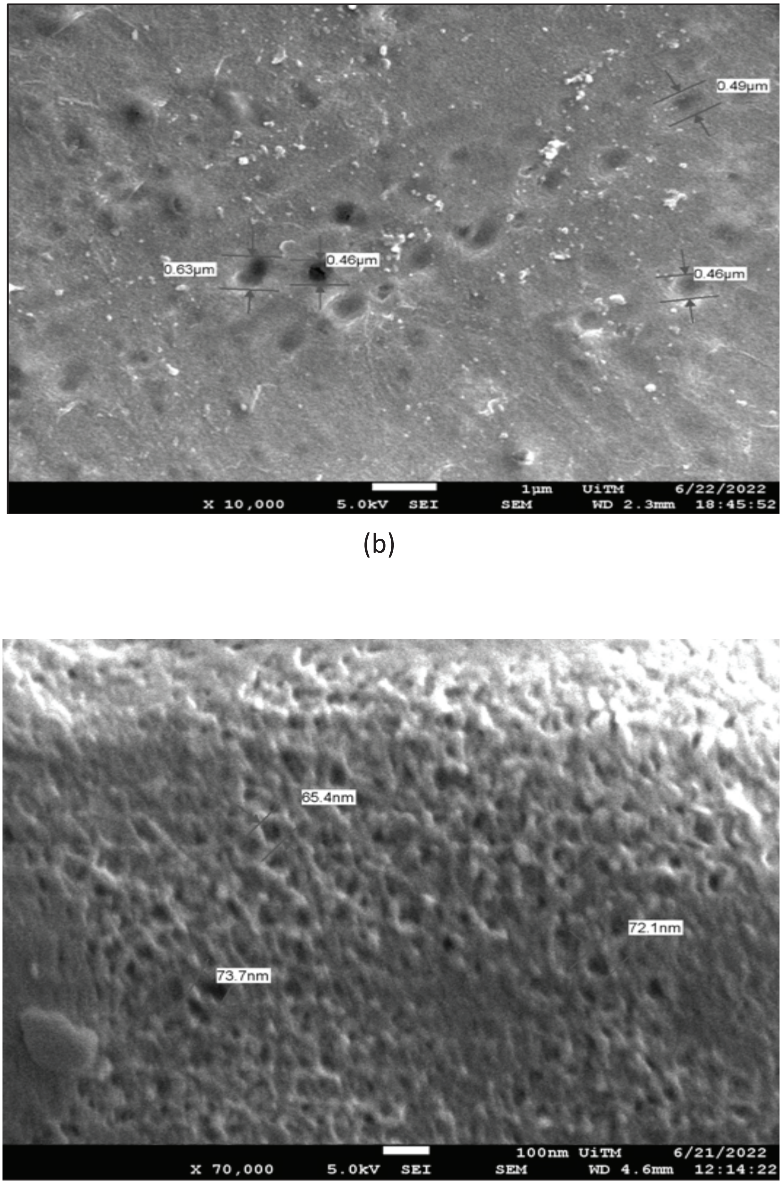

(b)

(c)

Figure 3: Surface images of membranes, (a) M1, (b) M2, (c) M3

CONCLUSION

It has been discovered that the quaternization process of chitosan was successfully conducted based on the obtained functional group, where this modification process enhanced the antifouling properties of the membrane. However, quaternization process fails to produce a positive charge membrane, and the subsequent crosslinking process with *TEOS* did not give a significant effect on improving the hydrophilicity of the membranes. However, the dense structure of membrane due to crosslinking process might result in a high degree of integral stability, with the additional benefit of providing more adsorption area in the heavy metal ion removal process.

ACKNOWLEDGMENT

The authors would like to thank Universiti Teknologi MARA (UiTM) for supporting this research through 600-RMC/GPK 5/3 (119/2020) grant.

REFERENCES

[1] Z. Cui, Y. Jiang, and R. W. Field, 2010. Chapter 1: Fundamentals of pressure-driven membrane separation processes, *Oxford*, UK.

[2] O. Labban, C. Liu, T. H. Chong, J. H. Lienhard, 2017. Fundamentals of low-pressure nanofiltration: Membrane characterization, modeling, and understanding the multi-ionic interactions in water softening. *Journal of Membrane Science*, 521, 18-32.

[3] A. Muñoz-Bonilla, M. Cerrada, and M. Fernández-García, 2014. Polymeric materials with antimicrobial activity, *The Royal Society of Chemistry Cambridge,* UK.

[4] G. Das, C. Y. Kim, D. H. Kang, B. H. Kim, H. H. Yoon, 2019. Quaternized polysulfone cross-linked n, n-dimethyl chitosan-based anion-conducting membranes. Polymers, 11(3), 1-13.

[5] R. L. Han, 2013. Preparation and characterization of positively charged quaternized chitosan/PEI composite nanofiltration membranes. *Advanced Materials Research*, 721, 45-48.

[6] T. M. M. Ways, W. M. Lau, and V. V. Khutoryanskiy, 2018. Chitosan its derivatives for application in mucoadhesive drug delivery, *systems. Polymers*, 10 (3), 1-37.

[7] R. A. A. Muzzarelli and R. Rocchetti, 1985. Determination of the degree of acetylation of chitosans by first derivative ultraviolet spectrophotometry. *Carbohydrate Polymers*, 5(6), 461-472.

[8] E. Curti, D. de Britto, and S. P. Campana-Filho, 2003. Methylation of chitosan with iodomethane: Effect of reaction conditions on chemoselectivity and degree of substitution. *Macromolecular Bioscience*, 3(10), 571-576.

[9] Z. Zakaria, S. K. Kamarudin, and S. N. Timmiati, 2019. Influence of graphene oxide on the ethanol permeability and ionic conductivity of QPVA-based membrane in passive alkaline direct ethanol fuel cells. *Nanoscale Research Letters*, 14(1), 1-18.

[10] X. Du, Y. Shi, V. Jegatheesan, I. U. Haq, 2020. A review on the mechanism, impacts and control methods of membrane fouling in MBR system. *Membranes (Basel)*, 10(2), 1-33.

[11] T. F. Speth, R. S. Summers, and A. M. Gusses, 1998. Nanofiltration foulants from a treated surface water. *Environmental Science & Technology*, 32(22), 3612-3617.

[12] J. Kucera, 2015. Reverse osmosis: Industrial processes and applications, second edition, *Scrivener Publishing LLC*,

[13] A. Koltuniewicz and A. Noworyta, 1994. Dynamic properties of ultrafiltration systems in light of the surface renewal theory. *Industrial & Engineering Chemistry Research,* 33 (7), 1771-1779.

[14] J. Berger, M. Reist, J. M. Mayer, O. Felt, N. A. Peppas, R. Gurny, 2004. Structure and interactions in covalently and ionically crosslinked chitosan hydrogels for biomedical applications. *European Journal of Pharmaceutics and Biopharmaceutics*, 57(1), 19-34.

[15] H. Y. Jung, R. K. Gupta, D. W. Seo, Y. H. Kim, C. M. Whang, 2002. Preparation and characterization of hybrid silica-poly(ethylene glycol) sonogel. *Bulletin of the Korean Chemical Society*, 23(6), 884-890.

[16] H. Cong, M. Radosz, B. F. Towler, Y. Shen, 2007. Polymer–inorganic nanocomposite membranes for gas separation. *Separation and Purification Technology*, 55(3), 281-291.

[17] N. A. Sulaiman, N. Z. K. Shaari, and N. A. Rahman, 2016. Removal of Cu (II) and Fe (II) ions through thin film composite (TFC) with hybrid membrane. *Journal of Engineering Science and Technology*, 11, 36-49.

[18] K. S. Norin Zamiah and A. S. Ahmed Qutb, 2021. Manganese in the source of groundwater in Malaysia and the method for the removal process: A review on the adsorption and membrane separation processes. *Malaysian Journal of Chemical Engineering & Technology,* 4(1), 1-7.

[19] K.-Y. Chen and S.-Y. Zeng, 2018. Fabrication of quaternized chitosan nanoparticles using tripolyphosphate genipin dual cross-linkers as a protein delivery system. *Polymers*, 10(11), 1-20.

[20] L. T. T. Nhung, I. Y. Kim, and Y. S. Yoon, 2020. Quaternized chitosan-based anion exchange membrane composited with quaternized poly polysulfone blend. *Polymers*, 12(11), 1-16.

[21] N. Z. K. Shaari, N. A. Rahman, and R. M. Tajuddin, 2012. Thin film composite membrane with hybrid membrane as the barrier layer: Preparation and characterization, in 2012 *IEEE (CHUSER*). 2012. Kota Kinabalu, Malaysia., 615-620.

[22] X. Wang, B. Liu, J. Ren, C. Liu, X. Wang, J. Wu, R. Sun, 2010. Preparation and characterization of new quaternized carboxymethyl chitosan/rectorite nanocomposite. *Composites Science and Technology,* 70(7), 1161-1167.

[23] R. P. Pandey and V. K. Shahi, 2013. Functionalized silica–chitosan hybrid membrane for dehydration of ethanol/water azeotrope: Effect of cross-linking on structure and performance. *Journal of Membrane Science*, 444, 116-126.

[24] E. Shokri, R. Yegani, S. Heidari, Z. Shoeyb, 2015. Effect of PE-g-MA compatibilizer on the structure and performance of HDPE/EVA blend membranes fabricated via TIPS method. *Chemical Engineering Research and Design*, 100, 237-247.

[25] S. Heidari, H. Etemadi, and R. Yegani, 2020. A comprehensive analysis of membrane fouling in microfiltration of complex linear macromolecules based on theoretical modeling and FESEM images. *Journal of Chemical Technology & Biotechnology*, 96, 1-55.

[26] A. Grenier, M. Meireles, P. Aimar, P. Carvin, 2008. Analysing flux decline in dead-end filtration. *Chemical Engineering Research and Design*, 86(11), 1281-1293.